Damping mechanisms in high-Q micro and nanomechanical string resonators

Schmid, Silvan; Jensen, K. D.; Nielsen, K. H.; Boisen, Anja

Published in:
Physical Review B Condensed Matter

Link to article, DOI:
10.1103/PhysRevB.84.165307

Publication date:
2011

Document Version
Publisher's PDF, also known as Version of record

Damping mechanisms in high-Q micro and nanomechanical string resonators

S. Schmid,* K. D. Jensen, K. H. Nielsen, and A. Boisen

Department of Micro- and Nanotechnology, Technical University of Denmark, DTU Nanotech, Building 345 East, DK-2800 Kongens Lyngby, Denmark

(Received 23 August 2011; published 4 October 2011)

Resonant micro and nanostrings were found to have extraordinarily high quality factors (Qs). Since the discovery of the high Qs of silicon nitride nanostrings, the understanding of the underlying mechanisms allowing such high quality factors has been a topic of several investigations. So far it has been concluded that Q is enhanced due to the high energy stored in the string tension. In this paper, damping mechanisms in string resonators are systematically investigated by varying the geometry and the tensile stress of silicon nitride microstrings. The measured quality factors are compared to an analytical model for Q based on bending-related damping mechanisms. It is shown that internal material damping is limiting the quality factor of narrow strings with a width of 3 μm. Q is strongly width dependent and clamping losses evidently seem to be the limiting damping mechanism for wider strings. It is further shown that Q is influenced by interference effects in the substrate and thus by the clamping of the macroscopic chip. A maximum quality factor of up to 7 million is presented for high-stress silicon nitride strings with a resonance frequency of 176 kHz.

DOI: 10.1103/PhysRevB.84.165307 PACS number(s): 85.85.+j, 46.40.Ff, 46.70.Hg, 62.40.+i

I. INTRODUCTION

The quality factor Q of a mechanical resonator is defined as the ratio of stored energy versus lost energy during one cycle of vibration. The higher the Q, the sharper the resonance peak and the more accurate the resonance frequency can be determined. A high Q is desired for applications of micro and nanomechanical resonators, e.g., as mass sensors, frequency references, or filters for signal processing. In the search for high-Q mechanical resonators, Verbridge *et al.*[1] have found that highly stressed silicon nitride nanostrings have extraordinarily high quality factors compared to corresponding cantilever beams in the same frequency range. They showed that Q is increasing for long strings and have obtained maximal Q values of over a million for 325 μm long nanostrings.[2]

In a similar study, the quality factors of polymeric SU-8 microcantilevers and microstrings were compared.[3] The measured quality factor of the prestressed strings was significantly larger than the specific viscoelastic material damping limiting Q of the singly clamped cantilevers. Q of the polymeric strings was also higher than the calculated theoretical limit given by thermoelastic damping (TED). By changing the tensile stress σ in the strings, it could be shown that Q was enhanced with increasing stress. Q was most sensitive to stress in the low-stress regime. It was argued that clamping losses could ultimately limit the quality factor. A positive effect of tensile stress on the quality factor has also been reported for silicon nitride nanostrings.[4] As distinguished from the SU-8 strings, surface related damping effects were thought to limit Q.

According to the observed enhanced quality factors of prestressed strings, exceptionally high quality factors have also been observed with stressed silicon nitride membranes,[5,6] the two-dimensional equivalent to the silicon nitride strings, which are being of particular interest in the field cavity optomechanics.[7]

Based on the findings made with SU-8 microstrings, an analytical model was derived describing the effect of stress on the quality factor. Dismissing the contribution of elongational damping mechanisms, the quality factor of a string can be described by[3]

$$Q_{\mathrm{str}} = 2\pi \frac{W_{\mathrm{tension}} + W_{\mathrm{bending}}}{\Delta W_{\mathrm{bending}}}, \tag{1}$$

where W_{tension} is the elastic energy stored in the string tension and $\Delta W_{\mathrm{bending}}$ and W_{bending} are the lost and stored energy, respectively, due to bending. It is obvious that Q_{str} is enhanced by the stored tensile energy. Assuming that the magnitude of the tensile prestress is dominating the mechanical behavior, the energy stored in the flexural bending can be neglected and the quality factor of a string can be written as[3]

$$\begin{aligned} Q_{\mathrm{str}} &\approx \frac{W_{\mathrm{tension}}}{W_{\mathrm{bending}}} Q_{\mathrm{bending}} \\ &\approx \frac{\frac{1}{2}\sigma A \int_0^L \left[\frac{\partial}{\partial x} u(x)\right]^2 dx}{\frac{1}{2} E I_z \int_0^L \left[\frac{\partial^2}{\partial x^2} u(x)\right]^2 dx} Q_{\mathrm{bending}}, \end{aligned} \tag{2}$$

where σ is the tensile stress, A is the cross-section area, L is the length, E is the Young's modulus, I_z is the geometrical moment of inertia, $u(x)$ is the bending mode shape, and Q_{bending} is the quality factor due to bending related damping mechanisms in the relaxed state. From Eq. (2), it can be seen that Q_{str} is a function of the tensile stress. This equation was solved analytically for an ideal sinusoidal bending mode shape of a string, thereby dismissing the local flexural bending near the clamping of the string.[3] Later, Unterreithmeier et al. have shown that it is crucial to include the local bending close to the clamping sites.[8] They calculated Eq. (2) numerically for a realistic bending mode shape. They were able to fit the computed values to the measured quality factors of silicon nitride nanostrings. They obtained a good fit based on a frequency-independent fit parameter (Q_{bending}), which they assigned to intrinsic material damping.

Compared to cantilevers or stress-free bridges, the resonance frequency of strings is not a function of the beam thickness. It is mainly defined by the length and the tensile stress. This allows the reduction of the string thickness and thus

the resonator mass without lowering the resonance frequency. Furthermore, the resonance frequency can be tuned by changing the tensile stress.[4] Resonant micro and nanostrings have since become of interest for applications demanding high-Q resonators, such as ultra precise displacement[9,10] or mass[11] measurements. Due to the high sensitivity of the resonance frequency to changes in tensile stress, resonant strings are also being used as chemical[12] or temperature[13,14] sensors. Furthermore, the simple mode shape makes strings particularly suitable for particle mass spectrometry.[15]

The application of string resonators is growing and the fundamental understanding of the damping mechanisms in strings is important for the future design and optimization of high-Q micro and nanomechanical string resonators. In this work, damping mechanisms of silicon nitride strings are systematically investigated by varying string length, thickness, width, and tensile stress. We further present an analytical model for the quality factor in prestressed strings based on flexural damping mechanisms.

II. ANALYTICAL MODEL

For an ideal string, the flexural rigidity is zero and the corresponding mode shape is sinusoidal. In reality, a micro or nanomechanical string consists of a beam with a specific flexural rigidity. If the tensile stress in such a doubly clamped beam is sufficiently large, that is when $\sigma \gg (n\pi)^2 Eh^2/(12L^2)$,[16] where n is the mode number and h is the beam thickness, the stress is dominating the mechanical behavior and the rigidity can be neglected. This simplification results in accurate modeling, e.g., of the eigenfrequency of a string. But the damping due to the flexural bending near the clamping is the dominant source of dissipation in string resonators[8] and has therefore to be taken into account in a model for the quality factor in strings.

In our model we assume that the string mode shape is sinusoidal except near the clamping where we replace it by the mode shape of a singly clamped cantilever of length L_c, as schematically shown in Fig. 1. The bending moment and thus the stored energy near the clamping in a sinusoidal mode shape is small and can be dismissed. It can thus simply be replaced by a different mode-shape function.

The mode-shape function of the string part is given by

$$w(x) = z_0 \sin\left(\frac{n\pi}{L}x\right), \tag{3}$$

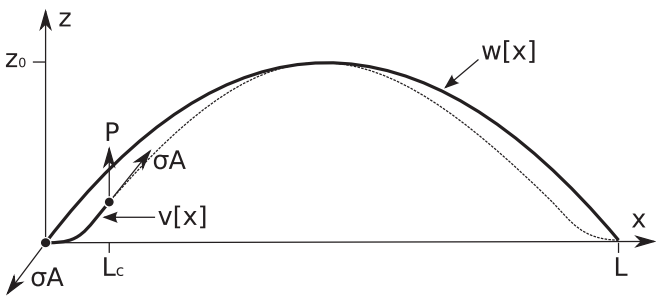

FIG. 1. Schematic drawing of a string bending mode shape including flexural bending near the clamping.

where z_0 is the maximal amplitude. The mode shape of the singly clamped cantilever beams near the clamping is[17]

$$v(x) = \frac{P}{6EI_z}x^2(3L_c - x), \tag{4}$$

where P is the point force acting on the cantilever tip in z direction. Assuming that $L_c \ll L$, it can be described as a function of the tensile force σA:

$$P = \frac{z_0 n\pi}{L}\sigma A. \tag{5}$$

At the contact point the two mode shapes need to have the same angle

$$\left.\frac{\partial w}{\partial x}\right|_{x=L_c} \approx \left.\frac{\partial w}{\partial x}\right|_{x=0} = \left.\frac{\partial v}{\partial x}\right|_{x=L_c}, \tag{6}$$

which together with Eq. (5) yields a term for the cantilever length

$$L_c = \sqrt{\frac{2EI_z}{\sigma A}}. \tag{7}$$

With Eqs. (4), (5), and (7), the energy stored in the cantilever bending near the string clamping can now be calculated.

$$\begin{aligned} W_{\text{bend-cant}} &= \frac{1}{2}EI_z\int_0^{L_c}\left(\frac{\partial^2 v}{\partial x^2}\right)^2 dx \\ &= z_0^2\frac{2^{\frac{3}{2}}\sqrt{\sigma AEI_z}(n\pi)^2}{6L^2}. \end{aligned} \tag{8}$$

Correspondingly, the energy stored in the rest of the string is given by

$$\begin{aligned} W_{\text{bend-str}} &= \frac{1}{2}EI_z\int_0^{L}\left(\frac{\partial^2 w}{\partial x^2}\right)^2 dx \\ &= z_0^2\frac{EI_z(n\pi)^4}{4L^3}. \end{aligned} \tag{9}$$

The flexural part $v(x)$ has a negligible impact on the total stored tensile energy in the string and therefore the calculation is exclusively based on $w(x)$:

$$\begin{aligned} W_{\text{tension}} &= \frac{1}{2}\sigma A\int_0^{L}\left(\frac{\partial w}{\partial x}\right)^2 dx \\ &= z_0^2\frac{\sigma A(n\pi)^2}{4L}. \end{aligned} \tag{10}$$

The quality factor of a string including flexural bending near the clamping assuming a rectangular cross section finally becomes

$$\begin{aligned} Q_{\text{str}} &= \left(\frac{W_{\text{bend-str}}}{W_{\text{tension}}} + \frac{2\,W_{\text{bend-cant}}}{W_{\text{tension}}}\right)^{-1} Q_{\text{bending}} \\ &= \left[\frac{(n\pi)^2}{12}\frac{E}{\sigma}\left(\frac{h}{L}\right)^2 + 1.0887\sqrt{\frac{E}{\sigma}}\frac{h}{L}\right]^{-1} Q_{\text{bending}}. \end{aligned} \tag{11}$$

From Eq. (11), it can be seen that the flexural bending part near the clamping is dominating. The contribution of the energy loss in the string bending becomes important for short lengths and higher mode numbers.

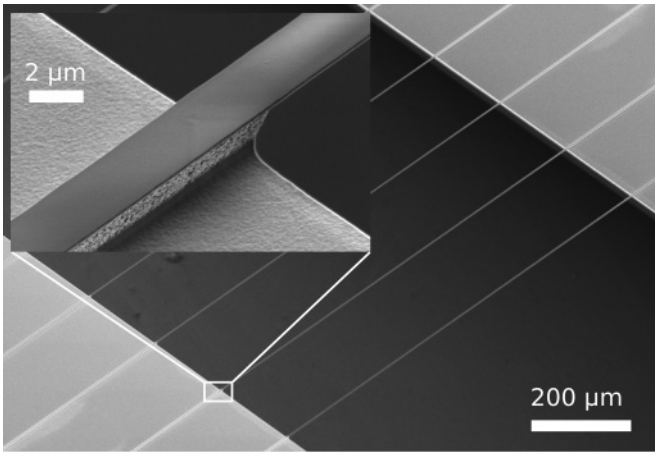

FIG. 2. SEM image of 157-nm thick, 3-μm wide high-stress silicon nitride strings.

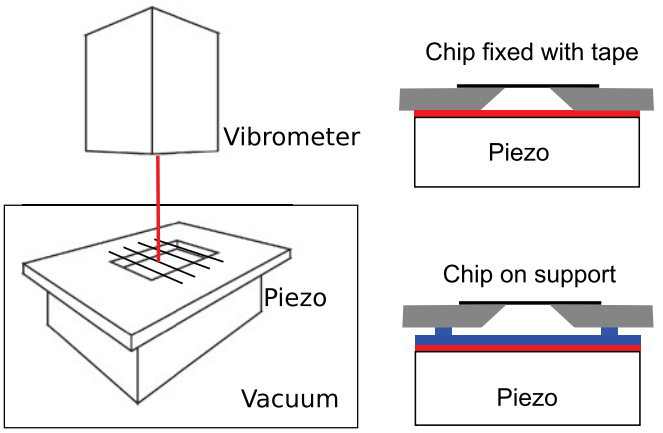

FIG. 3. (Color online) Schematic of the experimental setup. The string vibration was measured with a laser-Doppler vibrometer in high vacuum. The silicon chips holding the silicon nitride strings were actuated with a piezo. In one case, the chips were fixed by a double-sticky tape. In another case, the chips were placed on a silicon support that holds the chip on two bars.

III. EXPERIMENTAL

Micro and nanostrings are usually fabricated by surface micromachining, which results in under-etched anchor plates with the same thickness as the string. Clamping losses are maximal for this anchor design.[18] In order to exclude this effects due to under-etched anchor plates and thus to obtain largest possible Q values, the strings for this work were fabricated by means of bulk micromachining facilitating ideal clamping.

LPCVD (low-pressure chemical-vapor deposition) low-stress (silicon-rich) and high-stress (stoichiometric) silicon nitride was deposited on 350-μm thick silicon wafers. The strings were then defined on the front side by a dry etch step. The structured strings were covered with a PECVD (plasma enhanced chemical vapour deposition) silicon nitride layer and then released with a KOH etch from the back side. In a last step, the PECVD silicon nitride was selectively removed in buffered HF. The strings obtained with this process are shown in Fig. 2 and feature an ideal clamping. Strings with a thickness of 157, 177, and 340 nm were fabricated. The wafers were divided into individual chips of 10 mm $\times$ 7 mm containing 25 strings with widths of 3, 6, 14, 30, and 50 μm, five strings per width.

The strings were actuated with a piezo and read out with a laser-Doppler vibrometer (MSA-500 from Polytec GmbH). Two different methods were used for mechanically coupling the silicon chips to the piezo as schematically shown in Fig. 3. The quality factor of the first bending mode was determined by the ring-down method[19] at room temperature and a pressure below 1×10^{-5} mbar.

IV. RESULTS AND DISCUSSION

Frequency ratios of the second and third harmonic to the fundamental of 2.004 ± 0.002 and 3.027 ± 0.005, respectively, were measured for a 216-μm long and 340-nm thick low-stress beam, which represents a distinct stringlike behavior.[16] Material parameters such as the tensile prestress and Young's modulus were obtained by means of a model-based analysis. In order to apply the derived model (11), a value for Q_{bending} was obtained from the highest measured quality factors of singly clamped low-stress silicon nitride cantilevers with ideal clamping fabricated with the same process as the strings. All the material parameters used in this paper are listed in Table I. The subsequent calculations of Q_{str} are all based on these parameters.

The influence of air damping was investigated by measuring Q for different pressures. It was found that air damping is slightly limiting the Q values of the 3-μm thick, 1577-μm long, and 177-nm thick low-stress strings resonating at around 80 kHz. For all other strings, influence of air damping was found to be insignificant due to the higher resonance frequencies and the higher intrinsic damping.

In order to investigate the influence of the string geometry on the quality factor, strings with varying length and width were measured, see Fig. 4(a). In Fig. 4(b), the quality factors of similar strings with a different thickness are compared. The obtained Qs behave approximately linearly with length, an observation also made for silicon nitride nanostrings[1] and polymeric microstrings[3]. The measured quality factors are highest for the most narrow and thin strings. The 3-μm wide strings approach Q_{str}, which represents the limit due to intrinsic material damping. This confirms the results made with silicon nitride nanostrings with a width of 200 nm,

TABLE I. Material parameters of silicon nitride measured with doubly clamped strings and singly clamped low-stress silicon nitride cantilevers (558 μm $\times$ 100 μm $\times$ 549 nm) with ideal clamping.

Assumed material parameters	
mass density ρ	3000 kg/m^3
Poisson ratio ν	0.23
Obtained from doubly clamped strings	
low-stress σ	187 ± 13 MPa
high-stress σ	890 ± 59 MPa
Obtained from singly clamped cantilevers	
Young's modulus E	241 ± 4 GPa
Q_{bending}	~17 000

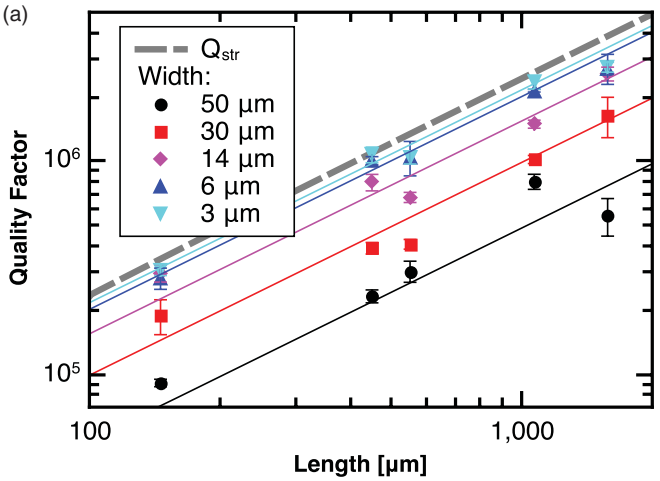

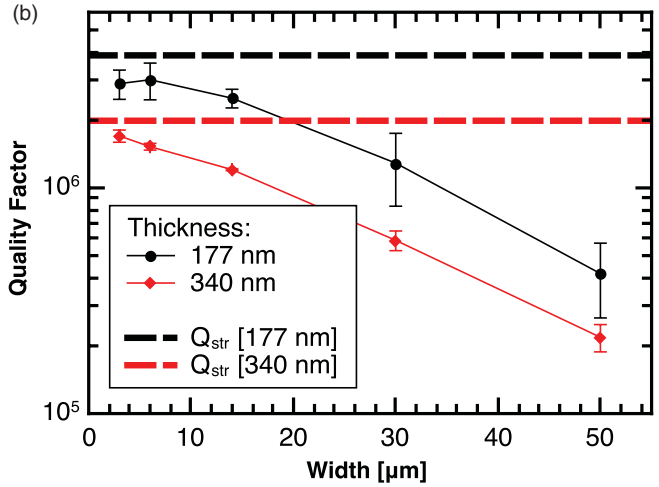

FIG. 4. (Color online) (a) Quality factors of 177-nm thick low-stress silicon nitride strings for varying length and width. The solid lines represent linear fits for quality factors with equal width. Every data point represents the average of more than five strings. (b) Average quality factors of 1577-μm long low-stress silicon nitride strings. The chips were fixed with double sticky tape. Every data point represents the average of more than five strings. The dashed line represents the calculated maximal quality factor due to intrinsic material damping Q_{str} (11).

which were dominated by frequency-independent material friction.[8] The width dependence of Q observed here can be explained by clamping losses. Clamping loss has been derived for singly[20] and doubly clamped[21] beam resonators and obeys the following rule:

$$Q_{\mathrm{clamp}} \propto \frac{L}{w}, \tag{12}$$

where w is the width. Thus the energy dissipation over the clamping is proportional to the beam width.

Other potential loss mechanisms such as TED and surface loss are being discussed subsequently. TED can be precisely calculated[22] and the resulting Qs are one order of magnitude higher than the measured values. Due to the string tension, these numbers would be even higher and consequently TED can be neglected. Surface losses have been thought to limit silicon nitride nanostrings.[4] The measured Q is higher for

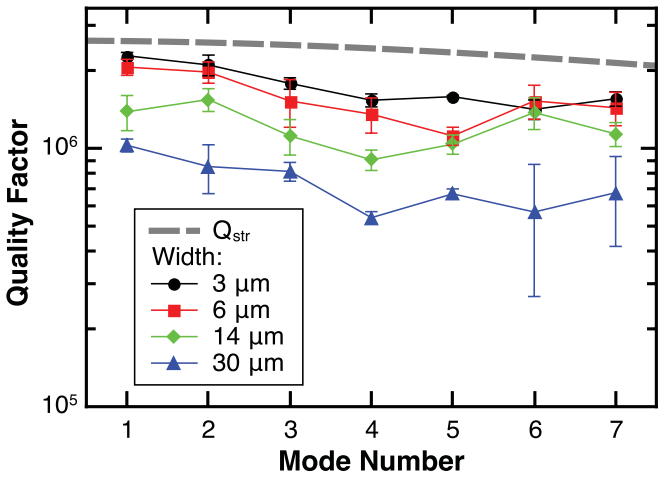

FIG. 5. (Color online) Quality factors of 1067-μm long low-stress silicon nitride strings for higher bending modes for varying width. Every data point represents the average of three strings. The dashed line represents the calculated maximal quality factor due to intrinsic material damping Q_{str} (11).

thinner strings [see Fig. 4(b)], in contrast to surface-loss models that predict an improvement of Q for thicker beams.[19,23] Furthermore, surface loss would be width independent. Hence, the measured data clearly indicate that surface losses are not limiting Q.

In Fig. 5, Q was measured for higher bending modes. According to the analytical model (11), Q is declining slightly for higher mode numbers. At higher modes, the local bending at the clamping is increased and the string has an increasing number of bends due to which more energy is dissipated. Beside the obvious strong width dependence, a minute variation of Q for higher bending modes can be noticed. The increase and decrease of Q for subsequent mode numbers can be interpreted as a result of interference of elastic waves that radiate into the substrate via the clamping. This effect has been described for a string resonator in the supplementary material of Ref. 8, and it was measured for silicon nitride membrane resonators.[24]

Q of the silicon nitride strings, in particular for the high-stress strings, varied from measurement to measurement. As for the observed variation of Q for higher bending modes, the values seemed to be influenced by interference effects with the substrate and thus by the fixation of the chip on the piezo. Therefore a silicon support was built on which the silicon chips containing the strings were placed. The support has two bars on which the chip is placed to allow the substrate more freedom to move, see Fig. 3. The results are shown in Fig. 6. For both, the low- and high-stress strings, the measured quality factors increase when placed on the silicon support instead of being taped down. The resonance frequencies did not change for the two different fixing methods. When placed on the holder, Qs of low-stress strings become width independent and reach the limit given by Q_{str}. By placing it on the holder, the influence of clamping losses seem to be efficiently reduced. The same procedure increases Qs for the high-stress strings, but the mechanical coupling to the substrate is still dominating Q over the effect of intrinsic material damping.

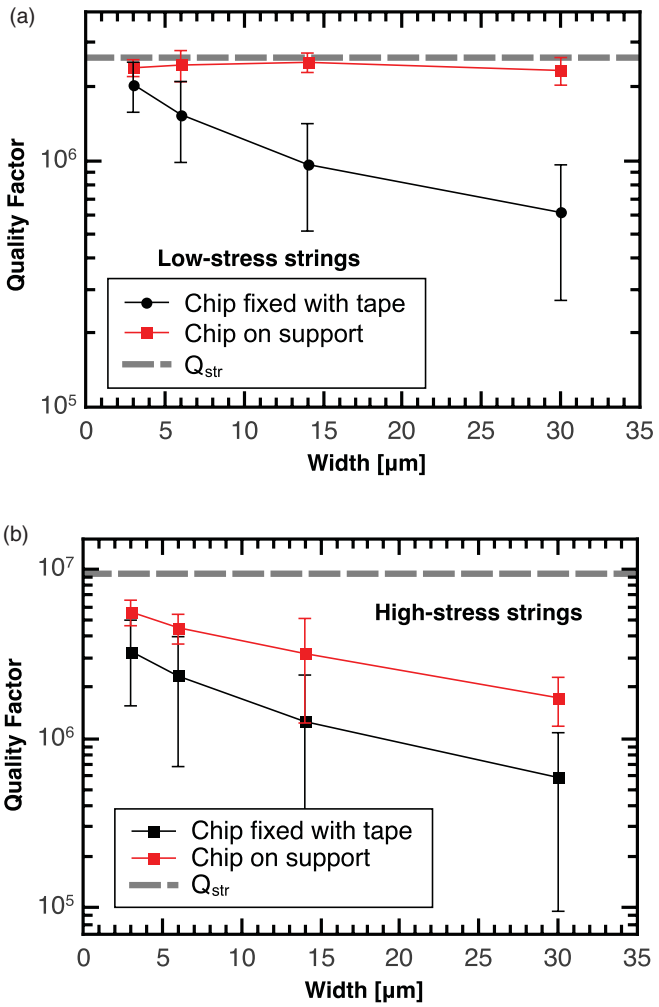

FIG. 6. (Color online) Comparison of the quality factors of silicon nitride strings when fixed with a double-sticky tape vs when placed on a support as depicted in Fig. 3. (a) The low-stress strings are 1067-μm long and 177-nm thick. (b) The high-stress strings are 1553-μm long and 157-nm thick. Every data point represents the average of more than 16 measurements with totally 10 strings. The dashed line represents the calculated maximal quality factor due to intrinsic material damping Q_{str} (11).

Figure 7 shows the highest measured quality factor of a high-stress silicon nitride string when the chip was mounted on the support. Therewith, a quality factor of almost 7 million was obtained at a resonance frequency of 176 kHz.

V. CONCLUSION

By systematically varying the geometry and the tensile stress, we have shown that the quality factor of silicon nitride strings is strongly width dependent. The mechanical coupling to the substrate is increasing with the string width and clamping losses are the dominating damping mechanism in most silicon nitride strings. For narrow low-stress strings, we could show, based on an analytical model, that intrinsic material friction starts to limit Q. According to the model, the effect of intrinsic material damping decreases in strings with increasing tensile stress. The high tension evidently exhibits increased mechanical coupling to the substrate and therefore clamping losses seem to dominate the high-stress strings.

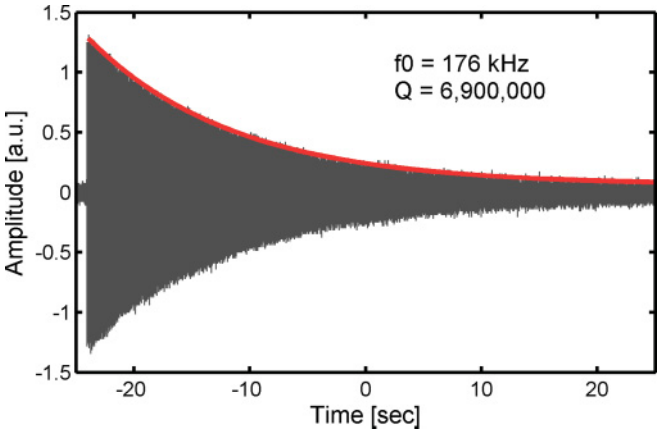

FIG. 7. (Color online) Ring-down curve of a 1553-μm long high-stress silicon nitride string placed on a support measured at room temperature.

Q was increased for both low-stress and high-stress strings when they were placed on a macroscopic chip holder that allows the substrate a certain freedom of movement. Thereby, clamping losses for wider low-stress strings could be canceled and the obtained Qs reached the material friction limit for all widths. Q of the high-stress strings also increased significantly up to a maximal value of 7 million. However, clamping losses remained dominant.

Consequently, quality factors of string resonators can be optimized by designing narrow strings in order to minimize clamping losses. The effect of intrinsic material friction can be minimized by increasing the tensile stress and by decreasing the string thickness. Beside the string geometry also the mounting of the chip has to be optimized in a way that least mechanical energy is lost. The obtained results are important for the design of high-Q string resonators. The finding that the macroscopic clamping of the chip influences Q is also of great importance for the clamping of high-Q silicon nitride membranes used in cavity optomechanics.

ACKNOWLEDGMENTS

The research leading to these results has received funding from the European Community's Seventh Framework Programme (FP7/2007-2013) under grant agreement No. 211464-2. We would like to thank Tom Larsen for the help with the SEM pictures.

*silvan.schmid@nanotech.dtu.dk

[1] S. S. Verbridge, J. M. Parpia, R. B. Reichenbach, L. M. Bellan, and H. G. Craighead, J. Appl. Phys. **99**, 124304 (2006).

[2] S. S. Verbridge, H. G. Craighead, and J. M. Parpia, Appl. Phys. Lett. **92**, 013112 (2008).

[3] S. Schmid and C. Hierold, J. Appl. Phys. **104**, 093516 (2008).

[4]S. S. Verbridge, D. Finkelstein Shapiro, H. G. Craighead, and J. M. Parpia, Nano Letters **7**, 1728 (2007).
[5]B. Zwickl, W. Shanks, A. Jayich, C. Yang, B. Jayich, J. Thompson, and J. Harris, Appl. Phys. Lett. **92**, 103125 (2008).
[6]D. J. Wilson, C. A. Regal, S. B. Papp, and H. J. Kimble, Phys. Rev. Lett. **103**, 207204 (2009).
[7]J. Thompson, B. Zwickl, A. Jayich, F. Marquardt, S. Girvin, and J. Harris, Nature (London) **452**, 72 (2008).
[8]Q. Unterreithmeier, T. Faust, and J. Kotthaus, Phys. Rev. Lett. **105**, 27205 (2010).
[9]J. Teufel, T. Donner, M. Castellanos-Beltran, J. Harlow, and K. Lehnert, Nat. Nanotechnology **4**, 820 (2009).
[10]M. LaHaye, O. Buu, B. Camarota, and K. Schwab, Science **304**, 74 (2004).
[11]A. Naik, M. Hanay, W. Hiebert, X. Feng, and M. Roukes, Nat. Nanotechnology **4**, 445 (2009).
[12]X. Huang, M. Manolidis, S. Jun, and J. Hone, Appl. Phys. Lett. **86**, 143104 (2005).
[13]A. Pandey, O. Gottlieb, O. Shtempluck, and E. Buks, Appl. Phys. Lett. **96**, 203105 (2010).
[14]T. Larsen, S. Schmid, L. Gronberg, A. Niskanen, J. Hassel, S. Dohn, and A. Boisen, Appl. Phys. Lett. **98**, 121901 (2011).
[15]S. Schmid, S. Dohn, and A. Boisen, Sensors **10**, 8092 (2010).
[16]A. Boisen, S. Dohn, S. S. Keller, S. Schmid, and M. Tenje, Rep. Prog. Phys. **74**, 036101 (2011).
[17]M. Bao, *Analysis and Design Principles of MEMS Devices* (Elsevier, 2005).
[18]S. Schmid, B. Malm, and A. Boisen, in *Proceedings of 24th International Conference on Micro Electro Mechanical Systems MEMS—2011, Cancun, Mexico* (IEEE, 2011), pp. 481–484.
[19]K. Y. Yasumura, T. D. Stowe, E. M. Chow, T. Pfafman, T. W. Kenny, B. C. Stipe, and D. Rugar, J. Microelectromech. Syst. **9**, 117 (2000).
[20]D. Photiadis and J. Judge, Appl. Phys. Lett. **85**, 482 (2004).
[21]M. C. Cross and R. Lifshitz, Phys. Rev. B **64**, 085324 (2001).
[22]R. Lifshitz and M. L. Roukes, Phys. Rev. B **61**, 5600 (2000).
[23]J. Yang, T. Ono, and M. Esashi, J. Microelectromech. Syst. **11**, 775 (2002).
[24]I. Wilson-Rae, R. Barton, S. Verbridge, D. Southworth, B. Ilic, H. Craighead, and J. Parpia, Phys. Rev. Lett. **106**, 47205 (2011).